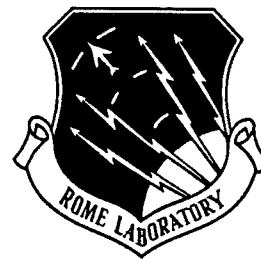


RL-TR-95-192
Final Technical Report
October 1995



RANDOM-ACCESS, PAGE-ORIENTED, STIMULATED ECHO OPTICAL CACHE MEMORY

SRI International

Ravinder Kachru and Yu Sheng Bai

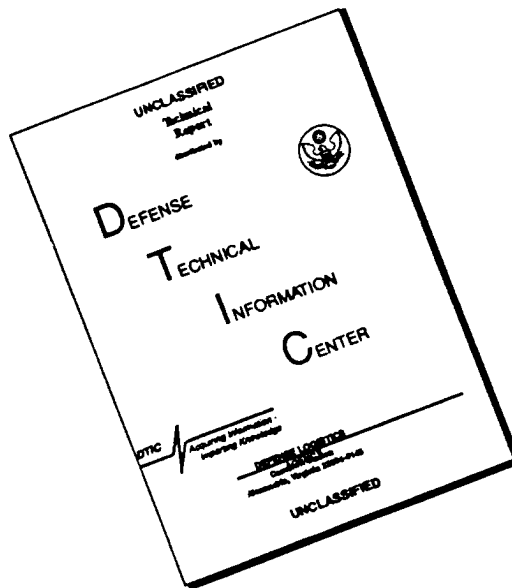
APPROVED FOR PUBLIC RELEASE; DISTRIBUTION UNLIMITED.

19960415 145

**Rome Laboratory
Air Force Materiel Command
Griffiss Air Force Base, New York**

DTIC QUALITY INSPECTED 1

DISCLAIMER NOTICE



THIS DOCUMENT IS BEST QUALITY AVAILABLE. THE COPY FURNISHED TO DTIC CONTAINED A SIGNIFICANT NUMBER OF PAGES WHICH DO NOT REPRODUCE LEGIBLY.

This report has been reviewed by the Rome Laboratory Public Affairs Office (PA) and is releasable to the National Technical Information Service (NTIS). At NTIS it will be releasable to the general public, including foreign nations.

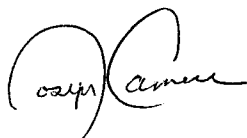
RL-TR-95-192 has been reviewed and is approved for publication.

APPROVED:



BERNARD J. CLARKE, Captain, USAF
Project Engineer

FOR THE COMMANDER:



JOSEPH CAMERA
Technical Director
Intelligence & Reconnaissance Directorate

If your address has changed or if you wish to be removed from the Rome Laboratory mailing list, or if the addressee is no longer employed by your organization, please notify RL (IRAP) Griffiss AFB NY 13441. This will assist us in maintaining a current mailing list.

Do not return copies of this report unless contractual obligations or notices on a specific document require that it be returned.

REPORT DOCUMENTATION PAGE			Form Approved OMB No. 0704-0188	
Public reporting burden for this collection of information is estimated to average 1 hour per response, including the time for reviewing instructions, searching existing data sources, gathering and maintaining the data needed, and completing and reviewing the collection of information. Send comments regarding this burden estimate or any other aspect of this collection of information, including suggestions for reducing this burden, to Washington Headquarters Services, Directorate for Information Operations and Reports, 1215 Jefferson Davis Highway, Suite 1204, Arlington, VA 22202-4302, and to the Office of Management and Budget, Paperwork Reduction Project (0704-0188), Washington, DC 20503.				
1. AGENCY USE ONLY (Leave Blank)		2. REPORT DATE October 1995		3. REPORT TYPE AND DATES COVERED Final ----
4. TITLE AND SUBTITLE RANDOM-ACCESS, PAGE-ORIENTED, STIMULATED ECHO OPTICAL CACHE MEMORY			5. FUNDING NUMBERS C - F30602-91-C-0102 PE - 62702F PR - 4594 TA - 15 WU - H2	
6. AUTHOR(S) Ravinder Kachru and Yu Sheng Bai				
7. PERFORMING ORGANIZATION NAME(S) AND ADDRESS(ES) SRI International 333 Ravenswood Avenue Menlo Park CA 94025-3493			8. PERFORMING ORGANIZATION REPORT NUMBER N/A	
9. SPONSORING/MONITORING AGENCY NAME(S) AND ADDRESS(ES) Rome Laboratory (IRAP) 32 Hangar Rd Rome NY 13441-4114			10. SPONSORING/MONITORING AGENCY REPORT NUMBER RL-TR-95-192	
11. SUPPLEMENTARY NOTES Rome Laboratory Project Engineer: Bernard J. Clarke, Captain, USAF/IRAP/ (315) 330-4581				
12a. DISTRIBUTION/AVAILABILITY STATEMENT Approved for public release; distribution unlimited.			12b. DISTRIBUTION CODE	
13. ABSTRACT (Maximum 200 words) This report describes a program of research to develop an innovative high-speed random-access optical cache memory. This innovation is based on a novel approach using time-domain-stimulated echo storage in smaller independent-frequency bins comprising the larger absorption bandwidth of rare-earth-doped crystals. The advantages of the approach are that memory can be stored in space, time, and frequency domain, allowing the tailoring of a flexible memory architecture to match those of the computational processor. We have instigated frequency, time, and space domain storage using a single frequency dye laser as an excitation source of optical pulses. Using Eu ³⁺ doped Y ₂ SiO ₅ crystal, we have stored and retrieved a 1.6 Kbit data stream, 40-μs long at a data rate of 40 Mbits/s in a single-frequency channel at one spatial location. By multiplying the total frequency channels available (at a single spatial spot of ~ 32), we infer a storage capacity of $\geq 5 \times 10^4$ bits per spatial spot, which is close to the theoretical storage density of 5×10^6 bits per spatial spot. We have achieved these results by solving the coherent saturation problem, caused by the limited frequency content of the data train, by using the pseudo-random biphasic modulation technique. Our results have demonstrated for the first time that the stimulated echo memory and, in particular, the time-frequency hybrid memory, is the memory of choice for the next generation of optical random access memory.				
14. SUBJECT TERMS Optical memories, Optical computers, Optical processing, Optical recording media			15. NUMBER OF PAGES 40 16. PRICE CODE	
17. SECURITY CLASSIFICATION OF REPORT UNCLASSIFIED	18. SECURITY CLASSIFICATION OF THIS PAGE UNCLASSIFIED	19. SECURITY CLASSIFICATION OF ABSTRACT UNCLASSIFIED	20. LIMITATION OF ABSTRACT UL	

CONTENTS

INTRODUCTION	1
BACKGROUND	3
Random Access Memory	5
Time-Frequency Domain Storage	6
Cache Memory System Architecture	6
EXPERIMENTAL RESULTS	11
CONCLUSIONS AND RECOMMENDATIONS	17
REFERENCES	18
APPENDIX	

INTRODUCTION

Sequential computers are fast approaching the fundamental physical limits of performance. Computers capable of parallel processing are being used to improve this performance and to increase the computational speed required for solving problems such as image analysis and image recognition. Parallel and array processors require fast, dense main and cache memory devices that can be accessed in parallel. Current memory technology cannot meet these requirements in terms of cost, compactness, or speed.

Computer memories are traditionally divided into five categories, listed here in increasing order of capacity and decreasing order of speed:

- (1) registers and microcontrol store
- (2) cache memory
- (3) main memory
- (4) disks
- (5) off-line storage.

In a computer, the cache memory stores prefetched data or instructions separately from the main memory. When the central processing unit (CPU) accesses memory, the cache tries to supply the data, instruction, or addresses requested. If it cannot do so, then the slower main memory must supply the data while the CPU waits. An important realization of this concept is pipeline or vector processing, in which the cache is preloaded with a sequence of instructions to be executed.

The goal of using a cache is not necessarily only to achieve optimal cache efficiency or even optimal processor performance. Rather, it is usually a more global objective, typically involving the optimization of system performance within certain cost, size, and power limits. Simply stated, the main system design goals should be the following.

- Minimize the probability of not finding a memory reference's target in the cache (miss rate = ratio of memory misses to total number of memory accesses).
- Minimize the time to access information in the cache.
- Minimize the delay caused by misses.
- Minimize the overhead costs of updating the main memory and maintaining coherency.

In this report, we describe the results of a program of research conducted by SRI International (SRI) directed toward the development of high-speed optical cache memory that uses the stimulated echo (SE) concept. SRI¹⁻⁵ and groups elsewhere⁶⁻⁸ have been investigating the physics of SE memory for many years. A fairly good understanding of the fundamental physics issues involved in the implementation of the SE memory concept has been established. The essence of SRI's memory concept is that information can be stored in space, time, and frequency domain (bins) by using SE. This freedom allows us to tailor a memory system so that it optimizes various memory parameters such as word size, parallel/serial access, input/output (I/O) speed, and access time to match those of the computer system using the cache memory.

The SE optical memory technique consists of using laser pulses to store and retrieve data from a suitable solid-state crystal cooled to low temperature. The SE memory requires the memory crystal to be at 4 to 20 K temperature. Therefore, the power requirements for cooling the memory crystal with a closed cycle refrigerator (which requires no replenishing of gases for a few years) are modest. Furthermore, the cache memory and the main large memory, which is needed in large intelligence databases and image processing systems, are generally located in a fixed facility.

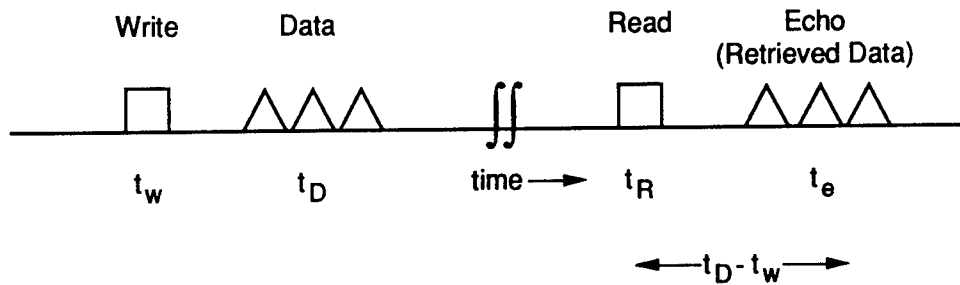
During the past year, we have for the first time quantitatively demonstrated that the stimulated echo memory can store information close to the theoretical estimate. Specifically, we have shown that $\geq 5 \times 10^4$ bits of digital information can be stored in a single spatial spot. Furthermore, we have demonstrated an input-output data speed of 40 Mbits/s using conventional acousto-optic modulators. Several key problems, such as frequency and amplitude stabilization of laser, long-term storage and coherent saturation problems were identified and solved before these important memory density and throughput results were achieved. However, an important breakthrough, which allowed the frequency spreading of data train, was the key to the success of our approach. The technique we discovered is the *pseudorandom sequence binary phase modulation*. Using this technique, which is described later in this report, a factor of 10 improvement in the memory density was achieved.

BACKGROUND

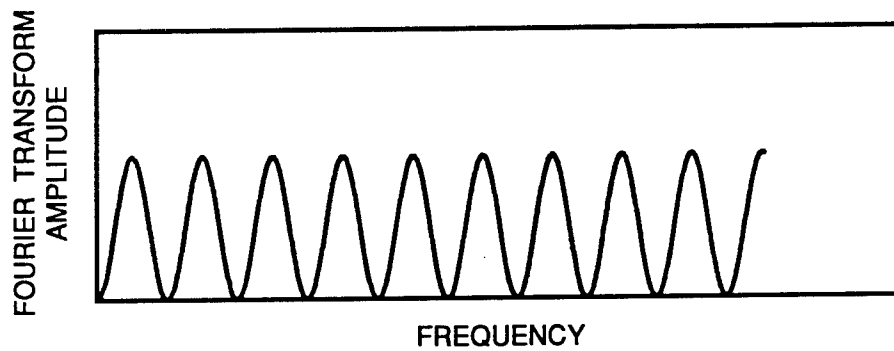
To illustrate the storage of information in the time domain, we use a simple diagram to describe the storage and retrieval of, first, a single bit and then, several bits of information. Figure 1(a) shows the temporal sequence of laser pulses (i.e., the write, data, and read pulses) required to store and retrieve several bits of serial information. The frequency of the laser excitation pulses is fixed to a particular color that is in resonance with a particular group of atoms within the larger absorption line of the memory crystal. We use a rare-earth ion doped in a crystal as our memory crystal. At low temperatures (4 to 30 K), the width of the frequency absorption of a single rare-earth ion is very small (a few kilohertz). However, the overall absorption width of the memory crystal is much larger (many gigahertz) because the rare-earth ions occupy a distribution of different sites in a crystal. Therefore, individual ions do not see the write and data pulses occurring at times $t_w = 0$ and t_D as two different pulses but rather as a complex pulse with a well-defined frequency Fourier transform.

For simplicity, Figure 1(b) shows the frequency Fourier transform (FT) of the write pulse and one of the data pulses from Figure 1(a). The FT of the three-pulse data pulse train shown in Figure 1(a) will be more complex than that shown in Figure 1(b). Figure 1(b) shows that the excitation spectrum is not uniform but is amplitude-modulated at frequencies proportional to the FT of the data pulse train. Therefore, the absorption of the memory crystal around the color of the laser itself will be modulated as a function of the absorption frequency. In other words, within a micron-sized pixel in the memory crystal, the serial bits representing information in the time domain are stored by a small group of atoms absorbing a particular color of light by Fourier transforming the temporal signal into frequency-domain absorption modulation. The information can be stored for many hours at low temperatures in a $\text{Eu}^{3+}:\text{YAlO}_3$ crystal.³

To read the information, we need only excite the memory crystal at time t_R with a single laser pulse of the same colors as the data and write pulses. The read pulse causes the atoms to take the inverse Fourier transform of the frequency population modulation, and the result is a coherent emission or echo by the memory crystal at time $t_R + (t_D - t_w)$. The echo pulse emitted by the memory crystal mimics the data pulse train, and the serial data can therefore be retrieved. Furthermore, the coherent nature of the emitted signal from the memory crystal allows the entire signal to be captured by a single detector at a high signal-to-noise ratio (S/N). This angular dependence of the signal is in contrast to that of the two-photon memory,⁹ where the fluorescence radiates into all angles and results in a smaller S/N.



(a) Temporal sequence of laser pulses



(b) Frequency Fourier transform of the write pulse and a single data pulse shown in (a)

CAM-330581-5A

Figure 1. Storage and retrieval of information.

We can begin to evaluate the potential storage density and read/write speeds for the stimulated echo memory approach by considering the restrictions placed on the laser pulses by the spectral properties of the absorbing atoms. The first requirement is that the laser pulses be separated by enough time that they are distinguishable. The minimum temporal separation between neighboring pulses is given by

$$\tau_p = \frac{1}{\pi\delta_I}$$

where δ_I (called the inhomogeneous linewidth) is the spread in the absorption frequencies of the atoms in the various sites in the sample.

The second requirement is that the last data pulse must arrive while the excited atomic dipoles can still compare it with the first data pulse. The maximum time between the first and last data pulse is given by

$$T_2 = \frac{1}{\pi\delta_H}$$

where δ_H (called the homogeneous linewidth) is the effective absorption linewidth of an atom at a specific site. T_2 is also called the dephasing lifetime. Its maximum value is the radiative lifetime of the excited state.

Thus, at most T_2/τ_p (or equivalently, δ_I/δ_H) bits of information can be stored in a single spot, and the read/write rate is just $1/\tau_p$. For Eu^{3+} doped in Y_2SiO_5 , the most optimum storage material, the ratio δ_I/δ_H is 5×10^6 , and $\tau_p = 1$ ps, obtaining a read/write rate of greater than 10^{10} bits/s and a storage density of more than 10^6 bits per spatial spot.

RANDOM ACCESS MEMORY

As discussed in the preceding section, stimulated echo (SE) memory is a high-speed, dense optical memory and is intrinsically massively parallel. In the standard implementation of the SE memory, long word sizes in the range of 10^4 to 10^5 bits emerge in a natural way to achieve the high-density optical storage. The long word size is reasonable and perhaps desirable for some random mass memory applications. However, in contrast, the cache memory application requires partitioning the memory into smaller subunits so that each memory location has the following features:

- (1) Word size should be smaller (16, 32, 64, 128... bits long), so that each memory location is randomly accessible for both reading and writing without affecting other locations
- (2) The contents of each memory location should in principle be independently erasable
- (3) Reading and writing to different memory locations simultaneously should be possible.

From the discussion in the preceding section, the standard implementation of the SE memory scheme evidently does not have the cache memory features listed above.

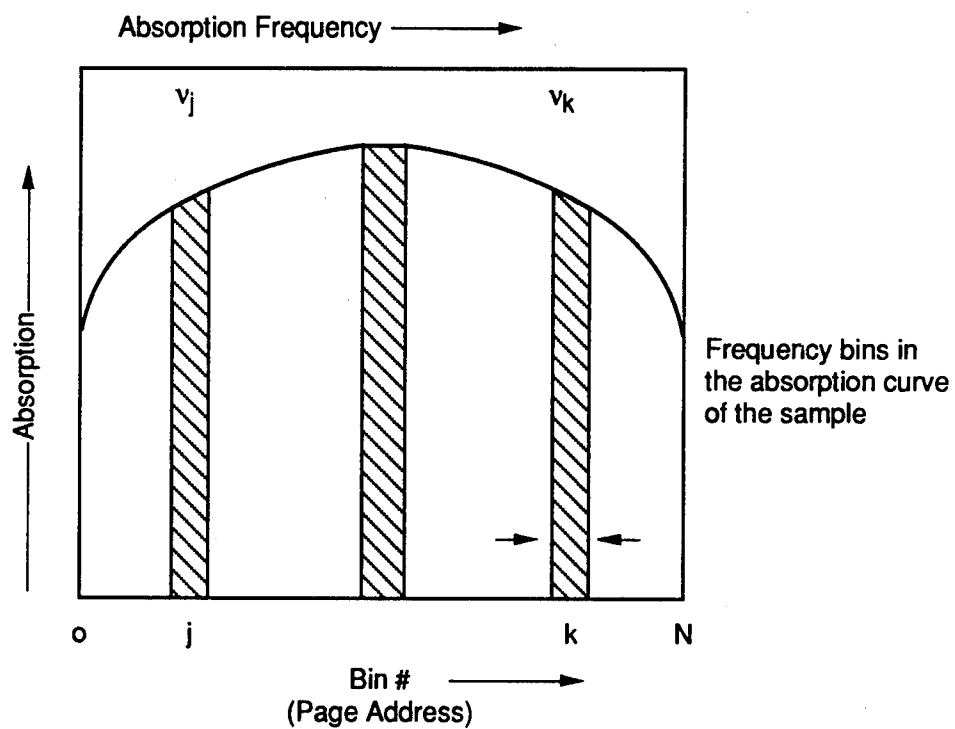
To address these cache memory features, we have developed a new data storage scheme that is, in essence, a hybrid of the time domain SE concept and the frequency domain hole-burning scheme. The basic new idea that we have developed is the partitioning of the absorption frequency domain into smaller bins, so that each frequency bin stores a smaller amount of information independently. The bins are distinguishable by their different absorption frequencies, and they are accessed by changing the laser frequency (color). However, information is still read and written using the stimulated echo concept (i.e., the time-domain pulse sequence).

TIME-FREQUENCY DOMAIN STORAGE

Because the SE memory can store 10^{12} bits/cm³, its true potential can be realized by storing information not only in the time domain but also in the frequency domain of a single pixel in the memory crystal. For example, as shown in Figure 2, the entire absorption frequency of the memory crystal can be subdivided into N frequency bins (colors), each of which can store several bytes of serial information. This storage can be accomplished by using a narrow linewidth laser and setting its frequency (color) to the center of one bin. The pulse sequence shown in Figure 1(a) now stores and retrieves the serial information at this frequency bin within a pixel.

CACHE MEMORY SYSTEM ARCHITECTURE

Efficient implementation of parallel algorithms in a parallel computer requires a memory device (cache and main memory) that can be accessed in parallel by all the processors. One of the most important aspects of the SE memory is its ability to record and retrieve data in parallel by simultaneously writing data to and reading data from both spatially resolved and frequency-resolved points in the crystal, so that the I/O bottlenecks inherent in the serial computer can be



CM-330581-14

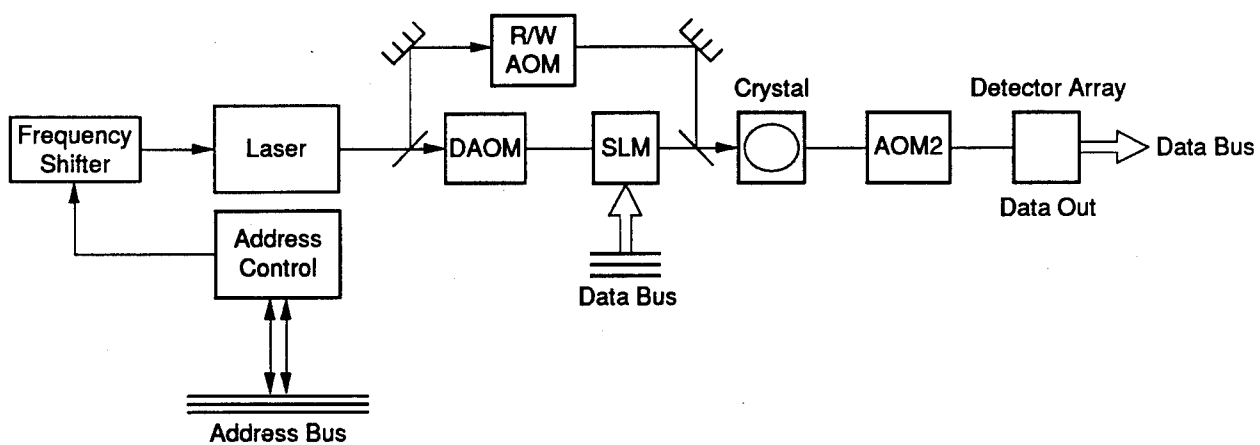
Figure 2. Division of absorption frequency spectrum into N frequency bins.

avoided. Here, we discuss how a stimulated-echo random-access cache memory records and retrieves data in parallel, using a two-dimensional page format and the spatial, time, and frequency domain storage aspects discussed above.

Figure 3 shows a possible random-access page-oriented memory scheme that achieves parallel I/O, high speed, and large memory density using existing optical components and the basic frequency segmentation scheme as outlined in Figure 2. Figure 2 shows how the absorption frequency of the memory crystal is divided into N smaller frequency bins. The main idea here is to store one $m \times m$ frame of data, containing m^2 words, in one frequency bin k centered around the frequency ν_k and width $\Delta\nu$. For simplicity, consider storage of one bit of information in one frequency bin. This idea is implemented in the memory scheme shown in Figure 3. The input electrical data are loaded into the spatial light modulator (SLM). A narrow frequency laser (<1 MHz bandwidth) is amplitude-modulated twice by an electro-optic modulator (EOM) or an acousto-optic modulator (AOM) at times $t_w = 0$ and $t = t_D$, to produce the write and data pulses shown in Figure 1(a). For concreteness, assume that $\Delta\nu = 10$ MHz, so that the widths of the write and data pulses, τ_w and τ_D , are ≥ 16 ns. Pulse widths of several microseconds are realistic.

Once loaded into the SLM, the data page can be loaded into any free frequency bin by selecting the frequency ν_k of the laser. During the data pulse, the two-dimensional image carrying the data page k produced by the SLM is imaged into the crystal, and, similarly during the write pulse, the uniformly illuminated image is input into the memory crystal. Two separate AOMs (or EOMs) are used to produce the write and data pulses, respectively, because the write and read pulses are not spatially modulated. In this way, a single page is recorded in a single frequency bin in the memory crystal.

For the next page of data, the frequency of the laser can be changed to ν_{k+1} or any available frequency bin and the write and data pulse cycle repeated. If the absorption width of the memory crystal is 10 GHz, then $N = 10 \text{ GHz} / \Delta\nu = 10^3$ bins. If we assume that m is 512, then the total number of bits per frame is 0.25×10^6 and the total number of bits in all frames is 0.25×10^9 bits. An entire page of data containing $\sim 10^6$ bits is read or written in parallel, achieving bit rates above 10^{10} bits/s, using existing optical components. Because the SE allows temporal domain storage, each frequency bin in each pixel can store several *bytes* of serial data. We estimate a storage density of 10^{12} bits/cm³, I/O throughput of 10^{10} bits/s, and access time of 10^9 bits/s. In addition, each page of data can be randomly accessed, and different pages of data can be read and written at the same time by using two separate lasers for reading and writing (not shown in Figure 3).



CM-330581-15

Figure 3. Stimulated echo cache memory schematic.

R/W and DAOM AOM's are the acousto-optic modulators used for producing the read/write and data pulses, respectively. AOM2 is used as an optical shutter to optically isolate the input excitation from the detector array.

To read any frame (j), we first switch the laser to the appropriate frequency ν_j . Then the read pulse is turned on at time $t = t_R$. The memory crystal then emits an echo pulse at time $t = t_R + t_{wD}$, where t_{wD} is the temporal separation between the data and write pulses, for all frequency bins. The echo pulse is in every way a replica of the original data frame (image) stored in frequency bin j . The echo pulse spatial intensity profile representing the bit pattern in any page can be read out by using a two-dimensional photodiode array detector. Because there is no interaction between any two frequency bins shown in Figure 2(b), writing one page and reading another page of data can be done by using two separate lasers for reading and writing.

We have described one of many possible memory schemes for recording and retrieving data in page format using the stimulated echo concept. The memory scheme outlined above is useful as a cache memory.

EXPERIMENTAL RESULTS

Stimulated photon echo¹⁰ memory, also known as coherent time-domain optical memory (CTOM),¹¹ offers the potential for ultrahigh storage density and ultrahigh data throughput rate. Like the frequency-domain optical memories (FOM)¹² such as persistent hole-burning, CTOM stores information in the spectral degree of freedom of an inhomogeneously broadened absorbing material in addition to the spatial addresses used in conventional two-dimensional optical memories. Unlike FOM, where the information is stored bit by bit directly in the frequency dimension, the information stored in CTOM is the Fourier transform of a structured data pulse, which is nominally an amplitude-modulated binary stream. The high speed inherent to the echo process enables CTOM to store and retrieve data at much higher rates than FOM. The storage density in a spatial address is a time-bandwidth (TB) product where T is the length of the data stream and B is the data rate. The theoretical limits on T and B are usually considered to be the homogeneous dephasing time (T_2) and the inhomogeneous bandwidth ($\Delta\nu$) of the storage material, respectively. In rare-earth-doped crystals, T_2 is typically $\sim 10^{-5}$ - 10^{-4} s and $\Delta\nu \sim 10^9$ - 10^{10} Hz, yielding maximal TB products of $\sim 10^4$ - 10^6 . Theoretically estimated maximal TB products up to 10^7 have been reported for some Eu^{3+} doped oxides.^{8,13} When dealing with a lower data rate, one can divide the inhomogeneous profile into frequency subchannels and hence obtain a similar storage density. The potential to store large data packages (~ 100 μs long) at a data rate of tens of megabits/second up to 10 gigabits/second makes the CTOM very attractive for many applications.

We have demonstrated for the first time that the experimental performance of the CTOM close to the theoretical estimates can indeed be obtained. In our experiment, a 1.6 kbit data package 40- μs long was stored at a data rate of 40 Mbit/s in a single-frequency channel at one spatial location. Multiplying the total frequency channels available (≥ 32), we obtained an inferred storage capacity of $\geq 5 \times 10^4$ bits per spatial spot.

A key factor for achieving such performance was the application of a novel spread-spectrum technique. In the initial stage of our experiment, we found that the length of a purely amplitude-modulated data stream was not simply determined by the dephasing time. Significant distortion on the retrieved data was observed long before T reached a fraction of the dephasing time. This phenomenon, of course, can easily be explained in terms of coherent saturation. For the echo to replicate the data, the excitations have to be kept in the unsaturated regime, i.e., input pulse area $A < 1$.¹ Since the pulse area of a purely amplitude-modulated pulse is

$$A \propto \int \sqrt{I(t)} dt, \quad (1)$$

there is a maximum constraint on the length of the pulse for a given laser intensity. For rare-earth-doped crystals with oscillator strength $\sim 10^{-8}$ and typical experimental conditions of ~ 10 -mW laser input and ~ 100 - μ m focal spots, we find that T is restricted to a few microseconds. Reducing the input intensity does not improve the situation by much because A is proportional to the square root of I . To overcome this problem, it is necessary to introduce some phase or frequency modulations to spread the data spectrum.

The importance of the phase modulation can be appreciated by a brief Fourier analysis of the problem. In the standard CTOM, three temporally separated laser pulses are used to excite an inhomogeneously broadened absorbing material, with pulses 1, 2, and 3 being the write, data, and read pulses, respectively. The information is stored on the frequency profile of the ground state population

$$\rho_{gg}(\omega) \propto |E_1(\omega) + E_2(\omega)|^2, \quad (2)$$

where $E_i(\omega)$ is the Fourier transform of the i th pulse and $\mu|E_i(\omega)|/\hbar < 1$ for all frequency components has been assumed.¹ Upon excitation by a delayed pulse 3 (read pulse), the sample emits an output signal (echo) with a Fourier transform

$$E_e(\omega) \propto E_1^*(\omega)E_2(\omega)E_3(\omega). \quad (3)$$

It is easy to see that the echo will replicate pulse 2 (data pulse) so long as the spectral product $E_1^*(\omega)E_3(\omega)$ is approximately flat over the bandwidth of $E_2(\omega)$. This condition can be satisfied if pulses 1 and 3 are sufficiently short.¹¹ It can also be satisfied if pulses 1 and 3 are (identically) frequency-chirped⁷ or phase-modulated¹⁴ so that their energy is evenly spread over the data bandwidth.

We point out here that for optimal storage, *the energy of the data pulse should also be spread evenly over the data bandwidth*. The energy distribution of a purely amplitude-modulated binary stream, in contrast, is usually just the opposite of this optimal condition. The bandwidth of the data is determined by that of a single bit. For example, the spectrum of a rectangular bit with bit-length τ is $[\tau \sin(x)/x]^2$, where $x = \Delta\omega \tau/2$, and $\Delta\omega$ is the Fourier frequency. Its energy is mostly confined within $\omega_0 \pm 2\pi/\tau$, where ω_0 is the carrier frequency. Because of the coherent superposition, the energy of a stream of purely amplitude-modulated bits tends to concentrate in some narrow spikes within the data bandwidth. In an extreme case, the spectrum of a data pulse with all the bits "on" is $[T \sin(x)/x]^2$, where $x = \Delta\omega T/2$, and the energy

is almost entirely confined within $\omega_0 \pm 2\pi/T$. The broad background of the spectrum outside this range only contributes to the sharp rising and falling edges of the data pulse. As is characteristic for the coherent superposition, the height of the peak at ω_0 is proportional to N^2 , where $N=T/\tau$ is the number of data bits. Thus, the absorbers within the peak can easily be saturated.

To avoid such coherent saturation, we can randomly modulate the phase of the data pulse so that the individual bits appear to be *incoherently superposed*. For demonstration purposes, we used a simple, well-known spread-spectrum technique in coherent communications: M-sequence pseudorandom biphas (0-180°) shifting (PRBPS).¹⁵ When the PRBPS and the amplitude modulation are at an identical rate, the spectrum of the data pulse is essentially an incoherent superposition of the spectra of all individual bits, with a relative fluctuation of ~ 1 . The ratio between the maximal peaks in the spectra of the data with and without PRBPS is thus $2N/N^2$, which is $\sim 1/500$ for $N = 1$ kbit. In other words, the saturation level increases by 500 times when PRBPS is applied.

Our experiment was performed on the 579.88-nm transition (7F_0 - 5D_0 , site 1) of a 0.1 at. % $\text{Eu}^{3+}:\text{YOS}$ (Y_2SiO_5) crystal¹⁶ at 2 K (Y_2SiO_5 crystal is sometimes referred to as YOS in literature. The transition was found to have an inhomogeneous broadening of 3.6 GHz [FWHM of $n(\omega)$], an optical density (OD) of 1.0 at the line center ($\ell = 7.5$ mm), and an oscillator strength of $\sim 5 \times 10^{-8}$. The frequency of the laser (Coherent 699-21) was tuned to one side of the inhomogeneous line where the linear absorption is $\sim 20\%$ ($\text{OD} = 0.1$). The two-pulse echo dephasing time measured under these conditions with very weak input pulse energy flux was found to be ≥ 800 μs . The optical pulse sequence was generated by acousto-optically modulating the CW dye laser, with pulse 1 (3) as the write (read) pulse and pulse 2 the data, which is a binary-encoded pulse train with a rate of 40 Mbit/s. The laser pulses are focused onto the sample with a beam waist ($1/e^2$ intensity radius) of 80 μm and a power of ~ 100 mW.

The phase of the data pulse was randomly modulated by PRBPS in addition to the amplitude modulation (Figure 4). The pseudorandom sequence generator is a 13-stage shift-register (8191 bits) with a XNOR feedback and runs synchronously with the amplitude modulation of the data at 40 Mbit/s. The bandwidth of the data was thus 80 MHz. The write and read pulses were frequency-chirped and had an identical duration of 6 μs . The frequency chirp was generated by ramping a voltage-controlled-oscillator VCO that drives the acousto-optical modulator (AOM) over a range of 44 MHz around the RF carrier frequency f_0 . The laser beam was double-passed through the AOM to compensate for the beam displacement associated with the frequency shift. As a result, the effective chirp on the optical pulses was 88 MHz.

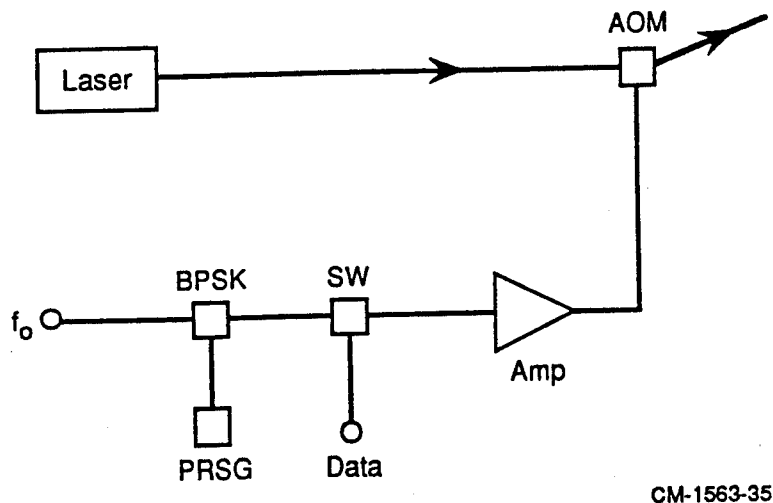
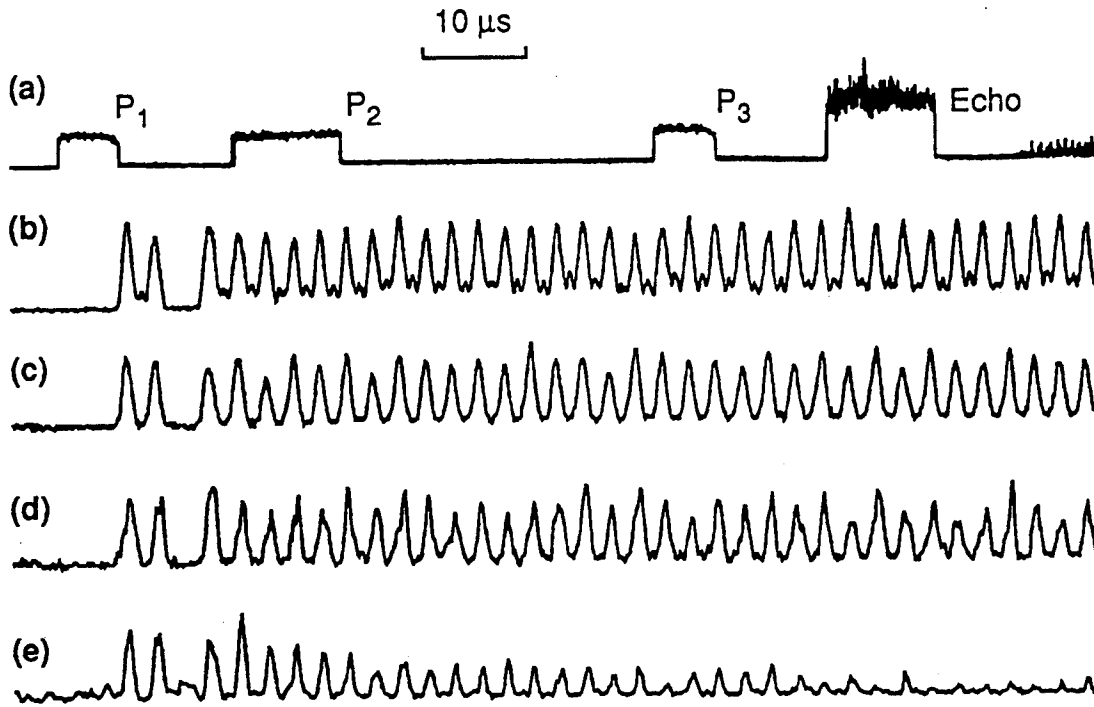


Figure 4. Schematic for PRBPS of the data pulse. PRSG: pseudorandom sequence generator; BPSK: biphas modulator; SW: RF switch; AMP: RF amplifier; AOM: acousto-optical modulator.

The echo signal was detected by a photomultiplier tube and recorded on a *single-event* basis by a digitizing oscilloscope. After each measurement, the laser was shifted by 110 MHz to a "fresh spot." The power of the observed echo signal is about 0.01% that of the input data pulse when t_{32} (storage time) was shorter than the excited state lifetime (2 ms). Echo signals with large t_{32} were about 30 times smaller.

Figure 5(a) shows the input pulse sequence and the echo signal (retrieved data) for a 10- μ s data pulse (400 bits). The input pulses were attenuated by $\sim 10^{-4}$. Figure 5(b) and Figure 5(c) show the input and retrieved data on an expanded time scale, respectively. Figure 5(d) shows the same data retrieved after about two minutes. The fluctuation is partly due to the shot noise. No noticeable signal degradation was observed after repeated reading for up to 10 times. The drastic effect of PRBPS (or the lack thereof) on the echo signal is shown in Figure 5(e), where PRBPS was off and the other experimental conditions were the same as those in Figure 5(c). The echo is completely distorted.



CM-1563-38

Figure 5. a) Input pulse sequence and echo signal (retrieved data). (b) P_2 on an expanded time scale ($0.2 \mu\text{s} : 10 \mu\text{s}$). The binary code is 10100010...10. (c) Echo signal on an expanded time scale. (d) Repeated retrieval after ~ 2 minutes. Vertical scale is expanded by a factor of 25; (e) Same as (b) with BPSK off. All signals were recorded on single-event basis.

Figure 6(a) shows a retrieved data pulse with $T = 40 \mu\text{s}$ (1.6 kbits). Figure 6(b) shows the retrieved data on an expanded time scale. The decay apparent on the profile of the retrieved data [Figure 6(a)] corresponds to a dephasing time of $\sim 400 \mu\text{s}$, which is now the sole limiting factor on the data length. This dephasing time is significantly shorter than that obtained with weak laser excitations ($\geq 800 \mu\text{s}$). The extra dephasing is believed to be due to excitation-induced instantaneous diffusion.¹⁷

As mentioned earlier, the separation between the frequency channels used in this experiment was 110 MHz, which resulted in about 32 frequency channels on the 3.6-GHz inhomogeneous width. Thus, the storage capacity inferred from this experiment is $\geq 5 \times 10^4$ bits per spatial spot. Since the length of the crystal is 7.5 mm, the equivalent storage density along the z-dimension is 1 bit per $0.15 \mu\text{m}$. Taking account of the total excitation volume we find that the storage density obtained here is 3.2×10^8 bits/cm³.

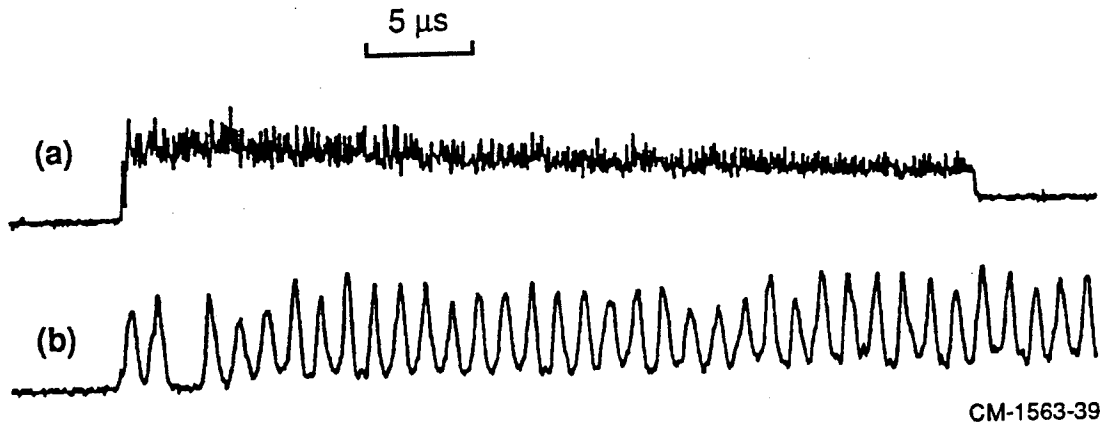


Figure 6. (a) Echo signal (retrieved data) from a 1.6-kbit data pulse.
 (b) Echo signal on an expanded time scale (0.2 μ s: 5 μ s).

It is to be noted that our reason to work with a very low absorption ($\alpha\ell \sim 0.25$) in this experiment is to minimize the excitation induced dephasing. As has been shown, the excitation induced dephasing is proportional to the absorption coefficient α and independent of the sample length ℓ .¹⁸ On the other hand, it is known that the echo efficiency is maximized at $\alpha\ell \sim 1$.¹⁹ In fact, echo efficiency 10 times as high as that obtained in our experiment is routinely obtained in most stimulated echo experiments. It is conceivable that we can get similar efficiency with an $\ell = 30$ mm crystal. In addition, the quantum efficiency of our photomultiplier tube is only 7%, which can be improved by a factor of 10 with existing technology. Taking account of these two factors, we could reduce the laser beam waist to 8 μ m and the input power to 1 mW, and still obtain a similar signal to noise ratio. The volume storage density thus calculated is 0.8×10^{10} /cm³, which sets the lower limit that can be obtained with existing technology.

CONCLUSIONS AND RECOMMENDATIONS FOR FURTHER RESEARCH

In conclusion, we have demonstrated time-domain storage of 1.6 kbits of data at a single-channel rate of 40 Mbit/s using stimulated photon echoes. Random phase-shifting of the amplitude-modulated data pulse was proved essential for the storage of long streams of bits. The inferred storage capacity, $\geq 5 \times 10^4$ bits per spatial spot, approaches the theoretical estimates and demonstrates the potential of this optical memory.

Although the potential of this memory has been experimentally demonstrated in our work, there are several aspects of this technique that need to be investigated. These are:

- 1) Storage and retrieval of information in all available frequency bins and the determinations of memory access time.
- 2) Signal-to-noise ratio as a function of the input-output data rate.
- 3) Storage and retrieval of information in parallel and
- 4) Demonstration of spatial memory addressing.

It is expected that the knowledge gained from systematic investigation of the topics outlined above will be useful in building a prototype memory.

REFERENCES

1. M. K. Kim and R. Kachru, Opt. Lett. **12**, 593 (1987).
2. M. K. Kim and R. Kachru, J. Opt. Soc. Am. **B4**, 305 (1987).
3. M. K. Kim and R. Kachru, Opt. Lett. **14**, 423 (1989).
4. M. K. Kim and R. Kachru, Appl. Opt. **28**, 2186 (1989).
5. S. Kröll, L. E. Jusinski, and R. Kachru, Opt. Lett. **16**, 517 (1991).
6. N. W. Carlson, W. R. Babbitt, and T. W. Mossberg, Opt. Lett. **8**, 623 (1983).
7. Y. S. Bai, W. R. Babbitt, and T. W. Mossberg, Opt. Lett. **11**, 724 (1986).
8. W. R. Babbitt and T. W. Mossberg, Opt. Commun. **65**, 185 (1988).
9. S. Hunter, F. Kiamilev, S. Esener, D. A. Parthenopoulos, and P. M. Rentzepis, Appl. Opt. **29**, 2058 (1990).
10. I. D. Abella, N. A. Kunit, and S. R. Hartmann, Phys. Rev. **141**, 391 (1966).
11. T. M. Mossberg, Opt. Lett. **7**, 77 (1982).
12. A. Szabo, U. S. Patent 3,896,420 (1975); W. E. Moerner, J. Molec. Elec. **1**, 55 (1985).
13. M. Mitsunaga, R. Yano, and N. Uesugi, Opt. Lett. **16**, 1890 (1991).
14. J. M. Zhang, D. J. Gauthier, J. Huang, and T. W. Mossberg, Opt. Lett. **16**, 103 (1991).
15. See, for example, *Principles of Modern Radar*, J. L. Eaves and E. K. Reedy, Eds. (Van Nostrand Reinhold, 1987), Chap. 15.
16. R. Yano, M. Mitsunaga, and N. Uesugi, Opt. Lett. **16**, 1890 (1991).
17. J. Huang, J. M. Zhang, A. Lezama, and T. W. Mossberg, Phys. Rev. Lett. **63**, 78 (1989).
18. Y. S. Bai and R. Kachru, Phys. Rev. B (12/92, to be published).
19. R. Friedberg and S. R. Hartmann, Phys. Lett. **37A**, 285 (1971).

APPENDIX

COHERENT TIME-DOMAIN DATA STORAGE USING SPREAD-SPECTRUM GENERATED BY RANDOM BIPHASE SHIFTING

COHERENT TIME-DOMAIN DATA STORAGE USING SPREAD-SPECTRUM GENERATED BY RANDOM BIPHASE SHIFTING

Y. S. Bai and R. Kachru
Molecular Physics Laboratory
SRI International
Menlo Park, CA 94025

ABSTRACT

We report time-domain data storage of up to 1.6 kbits at a rate of 40 Mbit/s in $\text{Eu}^{3+}:\text{YOS}$. Use of a pseudorandom biphase shifting technique to spread the data spectrum proved to be of critical importance in preventing saturation of the transition by the long data pulse train. The experimentally inferred storage capacity, $\geq 5 \times 10^4$ bits per spatial spot, plus the competitive single channel throughput rate, demonstrate the potential of this optical memory.

MP 92-225
October 28, 1992

Coherent time-domain optical memory (CTOM) [1], also known as stimulated photon echo [2] memory, offers the potential of ultrahigh storage density and ultrahigh data throughput rate. Like the frequency-domain optical memories (FOM) [3] such as persistent hole burning, CTOM stores information in the spectral degree of freedom of an inhomogeneously broadened absorbing material in addition to the spatial addresses used in conventional 2-D optical memories. Unlike FOM, where the information is stored bit by bit directly in the frequency dimension, the information stored in CTOM is the Fourier transform of a structured data pulse, which is nominally an amplitude-modulated binary stream. The high speed inherent to the echo process enables CTOM to store and retrieve data at much higher rates than FOM. The storage density in a spatial address is a time-bandwidth (TB) product where T is the length of the data stream and B is the data rate. The theoretical limits on T and B are usually considered to be the homogeneous dephasing time (T_2) and the inhomogeneous bandwidth ($\Delta\nu$) of the storage material, respectively. In rare-earth doped crystals, T_2 is typically $\sim 10^{-5}$ - 10^{-4} s and $\Delta\nu \sim 10^9$ - 10^{10} Hz, yielding maximal TB products of $\sim 10^4$ - 10^6 . Theoretically estimated maximal TB products up to 10^7 have been reported for some Eu^{3+} doped oxides [4,5]. When dealing with a lower data rate, one can divide the inhomogeneous profile into frequency subchannels [5] and hence obtain a similar storage density. The potential to store large data packages (~ 100 μs long) at a data rate of tens of megabits per second up to 10 gigabits per second makes the CTOM very attractive for many applications.

Here we report an experimental demonstration that performance of the CTOM close to the theoretical estimates can indeed be obtained. In our experiment, a 1.6 kbit data package 40 μs long was stored at a data rate of 40 Mbit/s in a single frequency channel at one spatial location. Multiplying the total frequency channels available (≥ 32), we obtained an inferred storage capacity of $\geq 5 \times 10^4$ bits per spatial spot.

A key factor for achieving such performance was the application of a novel spread-spectrum technique. In the initial stage of our experiment, it was found that the length of a purely amplitude-modulated data stream was not simply determined by the dephasing time. Significant

distortion on the retrieved data was observed long before T reached a fraction of the dephasing time. This phenomenon, of course, can easily be explained in terms of coherent saturation. For the echo to replicate the data, the excitations have to be kept in the unsaturated regime, i.e., input pulse area $A < 1$ [1]. Since the pulse area of a purely amplitude-modulated pulse is

$$A \propto \int \sqrt{I(t)} dt, \quad (1)$$

there is a maximum constraint on the length of the pulse for a given laser intensity. For rare-earth doped crystals with oscillator strength $\sim 10^{-8}$ and typical experimental conditions of ~ 10 -mW laser input and ~ 100 - μm focal spots, we find that T is restricted to a few microseconds. Reducing the input intensity does not improve the situation by much because A is proportional to the square root of I . To overcome this problem, it is necessary to introduce some phase or frequency modulations to spread the data spectrum.

The importance of the phase modulation can be appreciated by a brief Fourier analysis of the problem. In the standard CTOM, three temporally separated laser pulses are used to excite an inhomogeneously broadened absorbing material, with pulses 1, 2, and 3 being the write, data, and read pulses, respectively. The information is stored on the frequency profile of the ground state population

$$\rho_{gg}(\omega) \propto |E_1(\omega) + E_2(\omega)|^2, \quad (2)$$

where $E_i(\omega)$ is the Fourier transform of the i th pulse and $\mu|E_i(\omega)|/\hbar < 1$ for all frequency components has been assumed [1]. Upon excitation by a delayed pulse 3 (read pulse), the sample emits an output signal (echo) with a Fourier transform

$$E_e(\omega) \propto E_1^*(\omega)E_2(\omega)E_3(\omega). \quad (3)$$

It is easy to see that the echo will replicate pulse 2 (data pulse) so long as the spectral product $E_1^*(\omega)E_3(\omega)$ is approximately flat over the bandwidth of $E_2(\omega)$. This condition can be satisfied if

pulses 1 and 3 are sufficiently short [1]. It can also be satisfied if pulses 1 and 3 are (identically) frequency-chirped [6] or phase-modulated [7] so that their energy is evenly spread over the data bandwidth.

We point out here that for optimal storage, *the energy of the data pulse should also be spread evenly over the data bandwidth*. The energy distribution of a purely amplitude-modulated binary stream, on the other hand, is usually just the opposite of this optimal condition. The bandwidth of the data is determined by that of a single bit. For example, the spectrum of a rectangular bit with bit-length τ is $[\tau \sin(x)/x]^2$, where $x = \Delta\omega \tau/2$. Its energy is mostly confined within $\omega_0 \pm 2\pi/\tau$, where ω_0 is the carrier frequency. Because of the coherent superposition, the energy of a stream of purely amplitude-modulated bits tends to concentrate in some narrow spikes within the data bandwidth. In an extreme case, the spectrum of a data pulse with all the bits "on" is $[T \sin(x)/x]^2$, where $x = \Delta\omega T/2$, and the energy is almost entirely confined within $\omega_0 \pm 2\pi/T$. The broad background of the spectrum outside this range only contributes to the sharp rising and falling edges of the data pulse. As is characteristic for the coherent superposition, the height of the peak at ω_0 is proportional to N^2 , where $N=T/\tau$ is the number of data bits. Thus, the absorbers within the peak can easily be saturated.

To avoid such coherent saturation, we can randomly modulate the phase of the data pulse so that the individual bits appear to be *incoherently superposed*. For demonstration purposes, we used a simple, well-known spread-spectrum technique in coherent communications: M-sequence pseudorandom biphas (0-180°) shifting (PRBPS) [8]. When the PRBPS and the amplitude modulation are at an identical rate, the spectrum of the data pulse is essentially an incoherent superposition of the spectra of all individual bits, with a relative fluctuation of ~ 1 . The ratio between the maximal peaks in the spectra of the data with and without PRBPS is thus $2N/N^2$, which is $\sim 1/500$ for $N = 1$ kbit. In other words, the saturation level increases by 500 times when PRBPS is applied.

Our experiment was performed on the 579.88-nm transition (7F_0 - 5D_0 , site 1) of a 0.1 at. % $\text{Eu}^{3+}:\text{YOS}$ (Y_2SiO_5) crystal [9] at 2 K. The transition was found to have an inhomogeneous broadening of 3.6 GHz [FWHM of $n(\omega)$], an optical density (OD) of 1.0 at the line center ($\ell = 7.5$ mm), and an oscillator strength of $\sim 5 \times 10^{-8}$. The frequency of the laser (Coherent 699-21) was tuned to one side of the inhomogeneous line where the linear absorption is $\sim 20\%$ (OD = 0.1). The two-pulse echo dephasing time measured under these conditions with very weak input pulse energy flux was found to be ≥ 800 μs . The optical pulse sequence was generated by acousto-optically modulating the cw dye laser, with pulse 1 (3) as the write (read) pulse and pulse 2 the data, which is a binary-encoded pulse train with a rate of 40 Mbit/s. The laser pulses are focused onto the sample with a beam waist ($1/e^2$ intensity radius) of 80 μm and a power of ~ 100 mW.

The phase of the data pulse was randomly modulated by PRBPS in addition to the amplitude modulation (Fig. 1). The pseudorandom sequence generator is a 13-stage shift-register (8191 bits) with a XNOR feedback and runs synchronously with the amplitude modulation of the data at 40 Mbit/s. The bandwidth of the data was thus 80 MHz. The write and read pulses were frequency-chirped and had an identical duration of 6 μs . The frequency chirp was generated by ramping a VCO that drives the acousto-optical modulator (AOM) over a range of 44 MHz around the RF carrier frequency f_0 . The laser beam was double-passed through the AOM to compensate for the beam displacement associated with the frequency shift. As a result, the effective chirp on the optical pulses was 88 MHz.

The echo signal was detected by a photomultiplier tube and recorded on a *single-event* basis by a digitizing oscilloscope. After each measurement, the laser was shifted by 110 MHz to a "fresh spot". The power of the observed echo signal is about 0.01% that of the input data pulse when t_{32} (storage time) was shorter than the excited state lifetime (2 ms). Echo signals with large t_{32} were about 30 times smaller.

Fig. 2a shows the input pulse sequence and the echo signal (retrieved data) for a 10- μs data pulse (400 bits). The input pulses were attenuated by $\sim 10^{-4}$. Fig. b and Fig. 2c show the input

and retrieved data on an expanded time scale, respectively. Fig. 2d shows the same data retrieved after about two minutes. The fluctuation is partly due to the shot noise. No noticeable signal degradation was observed after repeated reading for up to 10 times. The drastic effect of PRBPS (or the lack thereof) on the echo signal is shown in Fig. 2e, where PRBPS was off and the other experimental conditions were the same as those in Fig. 2c. The echo is completely distorted.

Fig. 3a shows a retrieved data pulse with $T = 40 \mu\text{s}$ (1.6 kbits). Fig. 3b shows the retrieved data on an expanded time scale. The decay apparent on the profile of the retrieved data (Fig. 3a) corresponds to a dephasing time of $\sim 400 \mu\text{s}$, which is now the sole limiting factor on the data length. This dephasing time is significantly shorter than that obtained with weak laser excitations ($\gtrsim 800 \mu\text{s}$). The extra dephasing is believed to be due to excitation-induced instantaneous diffusion [10].

As mentioned earlier, the separation between the frequency channels used in this experiment was 110 MHz, which resulted in about 32 frequency channels on the 3.6-GHz inhomogeneous width. Thus, the storage capacity inferred from this experiment is $\gtrsim 5 \times 10^4$ bits per spatial spot. Since the length of the crystal is 7.5 mm, the equivalent storage density along the z-dimension is 1 bit per $0.15 \mu\text{m}$. Taking account of the total excitation volume we find that the storage density obtained here is $3.2 \times 10^8 \text{ bits/cm}^3$.

It is to be noted that our reason to work with a very low absorption ($\alpha\ell \sim 0.25$) in this experiment is to minimize the excitation induced dephasing. As has been shown, the excitation induced dephasing is proportional to the absorption coefficient α and independent of the sample length ℓ [11]. On the other hand, it is known that the echo efficiency is maximized at $\alpha\ell \sim 1$ [12]. In fact, echo efficiency 10 times as high as obtained in our experiment is routinely obtained in most stimulated echo experiments. It is conceivable that we can get similar efficiency with an $\ell = 30 \text{ mm}$ crystal. In addition, the quantum efficiency of our photomultiplier tube is only 7%, which can be improved by a factor of 10 with existing technology. Taking account of these two factors, we could reduce the laser beam waist to $8 \mu\text{m}$ and the input power to 1 mW, and still obtain a similar

signal to noise ratio. The volume storage density thus calculated is $0.8 \times 10^{10} / \text{cm}^3$, which sets the lower limit that can be obtained with existing technology.

In conclusion, we have demonstrated time-domain storage of 1.6 kbits of data at a single-channel rate of 40 Mbit/s using stimulated photon echoes. Random phase-shifting of the amplitude-modulated data pulse was proved essential for the storage of long streams of bits. The inferred storage capacity, $\geq 5 \times 10^4$ bits per spatial spot, approaches the theoretical estimates and demonstrates the potential of this optical memory.

This work was supported by the Rome Laboratories under Contract F30602-91-C-0102.

REFERENCES

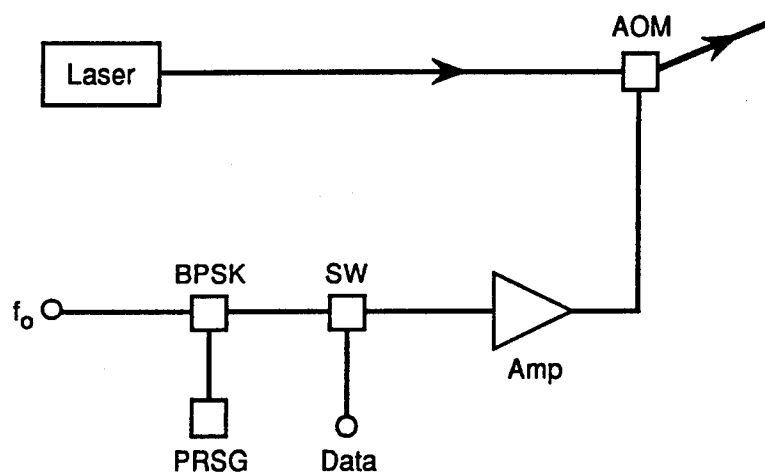
1. T. M. Mossberg, Opt. Lett. **7**, 77 (1982).
2. I. D. Abella, N. A. Kunit, and S. R. Hartmann, Phys. Rev. **141**, 391 (1966).
3. A. Szabo, U. S. Patent 3,896,420 (1975); W. E. Moerner, J. Molec. Elec. **1**, 55 (1985).
4. W. R. Babbitt and T. W. Mossberg, Opt. Commun. **65**, 185 (1988).
5. M. Mitsunaga, R. Yano, and N. Uesugi, Opt. Lett. **16**, 1890 (1991).
6. Y. S. Bai, W. R. Babbitt, and T. W. Mossberg, Opt. Lett. **11**, 724 (1986).
7. J. M. Zhang, D. J. Gauthier, J. Huang, and T. W. Mossberg, Opt. Lett. **16**, 103 (1991).
8. See, for example, *Principles of Modern Radar*, J. L. Eaves and E. K. Reedy, Eds. (Van Nostrand Reinhold, 1987), Chap. 15.
9. R. Yano, M. Mitsunaga, and N. Uesugi, Opt. Lett. **16**, 1890 (1991).
10. J. Huang, J. M. Zhang, A. Lezama, and T. W. Mossberg, Phys. Rev. Lett. **63**, 78 (1989).
11. Y. S. Bai and R. Kachru, Phys. Rev. B (12/92, to be published).
12. R. Friedberg and S. R. Hartmann, Phys. Lett. **37A**, 285 (1971).

FIGURE CAPTIONS

Figure 1. Schematic for PRBPS of the data pulse. PRSG: pseudorandom sequence generator; BPSK: biphase modulator; SW: RF switch; AMP: RF amplifier; AOM: acousto-optical modulator.

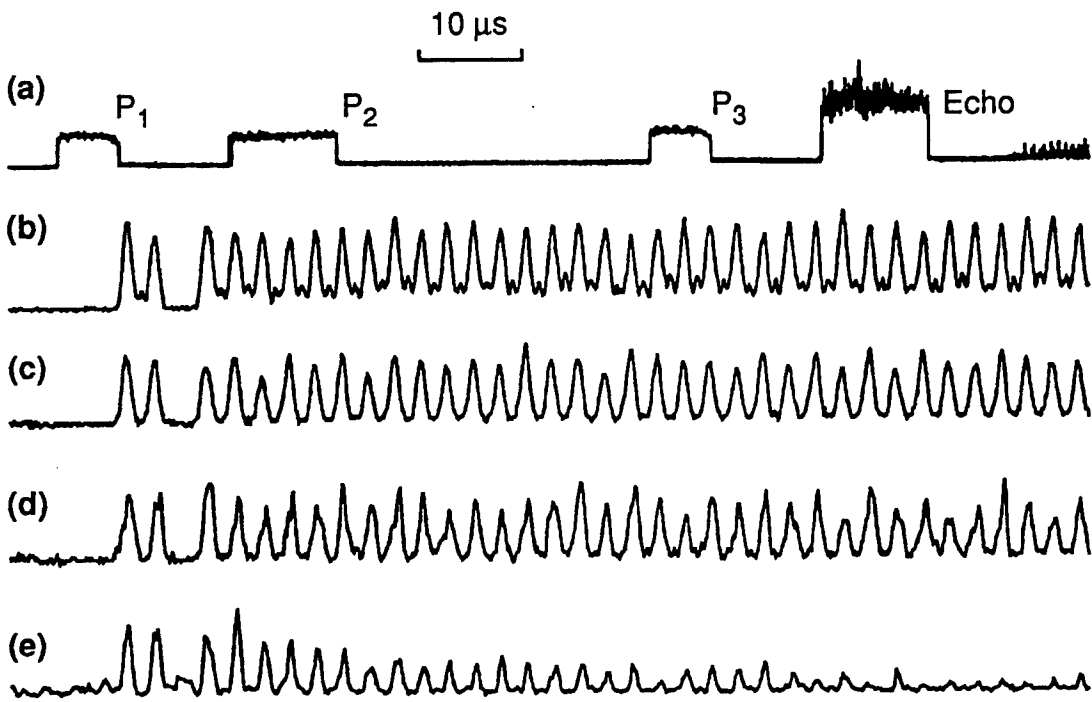
Figure 2. a) Input pulse sequence and echo signal (retrieved data). (b) P_2 on an expanded time scale ($0.2 \mu\text{s}$: $10 \mu\text{s}$). The binary code is 10100010...10. (c) Echo signal on an expanded time scale. (d) Repeated retrieval after ~ 2 minutes. Vertical scale is expanded by a factor of 25; (e) Same as (b) with BPSK off. All signals were recorded on single-event basis.

Figure 3. (a) Echo signal (retrieved data) from a 1.6-kbit data pulse. (b) Echo signal on an expanded time scale ($0.2 \mu\text{s}$: $5 \mu\text{s}$).



CM-1563-35

Figure 1



CM-1563-38

Figure 2

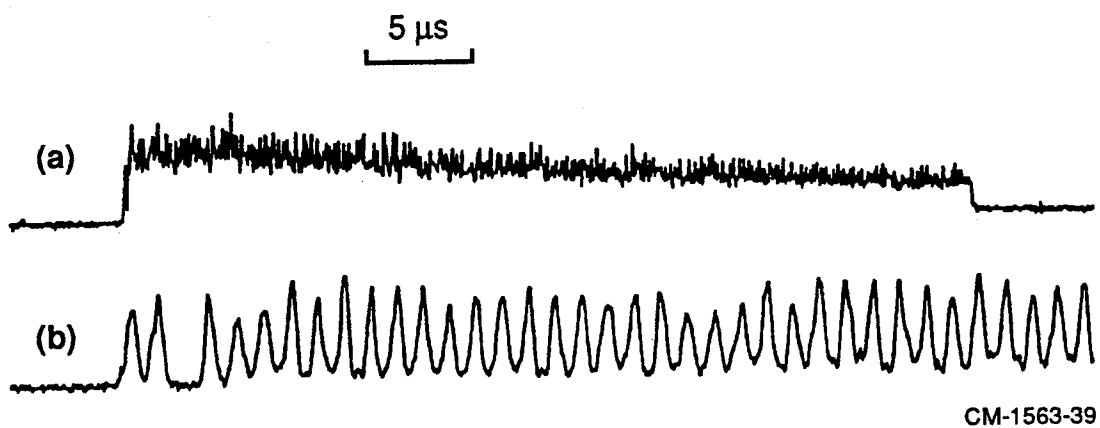


Figure 3

***MISSION
OF
ROME LABORATORY***

Mission. The mission of Rome Laboratory is to advance the science and technologies of command, control, communications and intelligence and to transition them into systems to meet customer needs. To achieve this, Rome Lab:

- a. Conducts vigorous research, development and test programs in all applicable technologies;
- b. Transitions technology to current and future systems to improve operational capability, readiness, and supportability;
- c. Provides a full range of technical support to Air Force Materiel Command product centers and other Air Force organizations;
- d. Promotes transfer of technology to the private sector;
- e. Maintains leading edge technological expertise in the areas of surveillance, communications, command and control, intelligence, reliability science, electro-magnetic technology, photonics, signal processing, and computational science.

The thrust areas of technical competence include: Surveillance, Communications, Command and Control, Intelligence, Signal Processing, Computer Science and Technology, Electromagnetic Technology, Photonics and Reliability Sciences.